

An Edible Rechargeable Battery

Ivan K. Ilic, Valerio Galli, Leonardo Lamanna, Pietro Cataldi, Lea Pasquale, Valerio F. Annese, Athanassia Athanassiou, and Mario Caironi*

Edible electronics is a growing field that aims to produce digestible devices using only food ingredients and additives, thus addressing many of the shortcomings of ingestible electronic devices. Edible electronic devices will have major implications for gastrointestinal tract monitoring, therapeutics, as well as rapid food quality monitoring. Recent research has demonstrated the feasibility of edible circuits and sensors, but to realize fully edible electronic devices edible power sources are required, of which there have been very few examples. Drawing inspiration from living organisms, which use redox cofactors to power biochemical machines, a rechargeable edible battery formed from materials eaten in everyday life is developed. The battery is realized by immobilizing riboflavin and quercetin, common food ingredients and dietary supplements, on activated carbon, a widespread food additive. Riboflavin is used as the anode, while quercetin is used as the cathode. By encapsulating the electrodes in beeswax, a fully edible battery is fabricated capable of supplying power to small electronic devices. The proof-of-concept battery cell operated at 0.65 V, sustaining a current of 48 μ A for 12 min. The presented proof-of-concept will open the doors to new edible electronic applications, enabling safer and easier medical diagnostics, treatments, and unexplored ways to monitor food quality.

1. Introduction

Over the last century, progress in health-care has almost doubled the average life expectancy of an individual, from 50 years to >80.^[1] Research in the medical sciences as well as advancements in food safety significantly contributed to improving the quality of life.^[2] The health of the gastrointestinal tract is an essential part of human wellbeing, however the diagnostic techniques used for gastrointestinal monitoring, such as gastroscopy and colonoscopy, are invasive and uncomfortable for the patient. Ingestible medical devices are revolutionizing the field, allowing some medical procedures like gastroscopies and colonoscopies to be replaced with less invasive pill-sized devices containing cameras and pH-sensors.^[3] Nevertheless, diagnostic procedures involving ingestible devices must still be performed under medical supervision due to the risk of device retention in human body, thus

significantly increasing the cost of operations and detracting from the value proposition of ingestible diagnostic devices. Fully edible electronics, made from food-grade materials that humans can safely digest, are promising to be an upgrade on their ingestible counterparts.^[4] A recent focus on green and edible electronics^[5,6] has laid the groundwork for edible medical devices which could be administered without direct medical supervision. The value of edible electronics is not solely limited to diagnostic devices for internal medicine, as an edible sensor or transmitter could find numerous applications in areas of food safety and sustainability by providing real-time data about food quality.^[7]

While the field of edible electronics is still in its infancy, researchers in recent years have produced several devices that fit the criteria of a fully edible electronic device. For example, Wang et al. developed an electrochemical sensor capable of detecting biologically relevant small molecules such as catechol, uric acid, ascorbic acid, dopamine, and acetaminophen.^[8] Jiang et al. developed an edible pH sensor, a radio frequency filter, and a microphone.^[9] More recently, Caironi and colleagues developed an edible defrosting sensor^[10] and an edible pill for intrabody communication.^[11] Recent advances in transistors based on natural dyes,^[12,13] and honey-gated transistors,^[14] demonstrate the feasibility of fully edible circuits in the near future. These examples of edible sensors and edible active electrical components are extremely encouraging to the prospect of designing more complex edible electronic systems.


I. K. Ilic, V. Galli, L. Lamanna, P. Cataldi, V. F. Annese, M. Caironi
Center for Nano Science and Technology @PoliMi
Istituto Italiano di Tecnologia
Via R. Rubattino, 81, Milan 20134, Italy
E-mail: mario.caironi@iit.it

V. Galli
Department of Physics
Politecnico di Milano
Piazza Leonardo da Vinci, 32, Milan 20133, Italy

L. Lamanna
Department of Engineering for Innovation
Campus Ecotekne
University of Salento
Via per Monteroni
Lecce 73100, Italy

P. Cataldi, A. Athanassiou
Smart Materials
Istituto Italiano di Tecnologia
via Morego 30, Genova 16163, Italy

L. Pasquale
Materials Characterization Facility
Istituto Italiano di Tecnologia
via Morego 30, Genova 16163, Italy

 The ORCID identification number(s) for the author(s) of this article can be found under <https://doi.org/10.1002/adma.202211400>.

© 2023 The Authors. Advanced Materials published by Wiley-VCH GmbH. This is an open access article under the terms of the Creative Commons Attribution License, which permits use, distribution and reproduction in any medium, provided the original work is properly cited.

DOI: 10.1002/adma.202211400

That being said, stable operation of edible electronic systems will require a reliable power source, which should also be edible. Electrochemical power sources, such as supercapacitors and batteries, can store energy as an electrical double layer or via redox reactions that occur at different potentials at opposite electrodes, respectively. Unfortunately, edible supercapacitors^[15–17] are not suitable as power sources due to their modest energy density and changing operational voltage. For edible applications, batteries would be a preferred power source as they can deliver current at defined potential. Fuel cells could be an alternative to batteries, and there has already been an exciting report of an edible fuel cell, which operated by burning ethanol, but the low volumetric energy density makes it unsuitable at present to power edible electronics.^[18]

Commercial Li-ion batteries, which power most portable electronic devices today, undergo a reduction of lithium metal oxides at the cathode and an oxidation of lithiated graphite at the anode during discharge, supplying power to an external circuit.^[19] However, commercial Li-ion batteries and other battery technologies (e.g., lead-acid batteries) are not suitable to power edible electronics as they contain toxic materials. To create edible batteries, the inspiration can be drawn from nature, as living organisms use similar redox pairs to power biochemical machines, such as enzymes. For example, respiratory complex I, a part of the respiratory chain, is powered by such a pair of redox reactions. While nicotinamide adenine dinucleotide (NAD) gets oxidized from NADH to NAD⁺ releasing electrons, ubiquinone gets reduced from quinone to hydroquinone form.^[20] Therefore, we postulate that naturally occurring, non-harmful redox pairs can be exploited to form edible batteries. To our knowledge, there has been only one report of an edible non-rechargeable battery by Bettinger et al., which utilized melanin as the anode and manganese oxide as the cathode.^[21] The battery operated as manganese oxide was reduced and melanin oxidized. However, manganese oxide can only be consumed in small amounts as an adequate daily intake of manganese is 3 mg, ≈50 μg per kg of body weight.^[22] Therefore, the charge these batteries can deliver is rather limited, and there is a great need to develop new batteries using materials with higher edibility. Furthermore, developing rechargeable batteries is essential in green electronics since it allows them to be reused when the application permits (e.g., food monitoring), thereby significantly reducing waste.

In this paper, we present the first edible rechargeable battery based only on organic redox-active materials. All the materials used in the formation of the battery are common food ingredients and additives that humans can eat without harm in large amounts, >100 mg per day. First, we prepared a composite of redox-active food additives and ingredients with activated carbon, a conductive food additive. This allows electrons to flow to and from the redox-active centers. Upon testing the electrochemical performance of these composites, we established two alternatives for cathode and anode materials. We chose the highest and the lowest redox reduction potential materials, namely riboflavin (vitamin B₂) and quercetin, and assembled the battery using edible current collectors and packaging. Such a battery can be used to power edible electronic devices operating outside the human body, as well as those operating inside, once the packaging is adjusted for the application. While

rechargeable properties of the battery might not be useful for short-lived applications inside the human body, edible devices operating outside the human body can be recharged, prolonging their lifetime. This long-sought achievement not only enables the development of edible electronics, but can also pave the way for the replacement of commercial batteries in ingestible devices, reducing their risk upon ingestion.

2. Results and Discussion

Redox-active food additives and ingredients, primarily small molecules, have low electrical conductivities and cannot be used alone as electrodes of the battery. To solve this issue, we mixed them with activated carbon (AC, E 153) to enable electron transport to and from redox centers. Two redox-active food additives were tested, indigo carmine (IC, E 132)^[23] and riboflavin (RF, E 101),^[24] as well as two food ingredients, quercetin^[25] (Q, a flavonoid found in food, e.g., capers) and ellagic acid (EA, polyphenol common in food, e.g., pomegranate).^[26] The discussion on the edibility of these compounds, as well as all the other materials used in the battery, can be found in the Supporting Information (2. Edibility of the materials). The composites were made by mixing the redox molecules with activated carbon in an appropriate solvent. IC, RF, and Q are soluble in water, but a water-ethanol mixture was used to facilitate the dispersion of activated carbon. As EA is more soluble in ethanol than in water, pure ethanol was used to prepare this composite.

The small molecules form a tight composite with activated carbon, as they get adsorbed on the carbon's surface. Nitrogen physisorption measurements (Figure S1, Supporting Information) confirm the blockage of the carbon pores by small molecules. Scanning electron microscopy micrographs (Figure S2, Supporting Information) and complementary energy dispersive X-ray mapping (Figure S3 and Table S1, Supporting Information) indicate an absence of small molecule aggregates pointing to high homogeneity of the samples. Detailed discussions of these measurements can be found in Supporting Information (6. Characterization of small molecule composite with activated carbon).

The composites were incorporated into the electrodes by binding them with ethyl cellulose (E 462), a food additive soluble in ethanol but not in water. Food-grade decorative gold (E 175) laminated onto ethyl cellulose was used as the current collector due to gold's high electrical conductivity.

Two redox-active materials were tested as possible active components in anodes: IC and RF (**Figure 1a**). IC is a food coloring with no biological function as a redox mediator. Nevertheless, IC was previously used as a redox-active molecule for energy storage.^[27–29] On the other hand, RF is a natural redox cofactor that is well known as vitamin B₂, and it is a widespread food supplement. It was previously used as cathode material in Li-ion batteries and anode material in aqueous redox flow batteries.^[30,31] Both IC and RF exhibit redox reactions at potentials slightly above the reduction potential of water, 0 V versus standard hydrogen electrode (SHE) at pH = 0, which makes them good choices as anode materials in aqueous electrolytes. Aqueous electrolytes will be used to form edible batteries as water is the electrolyte of natural redox-active systems.

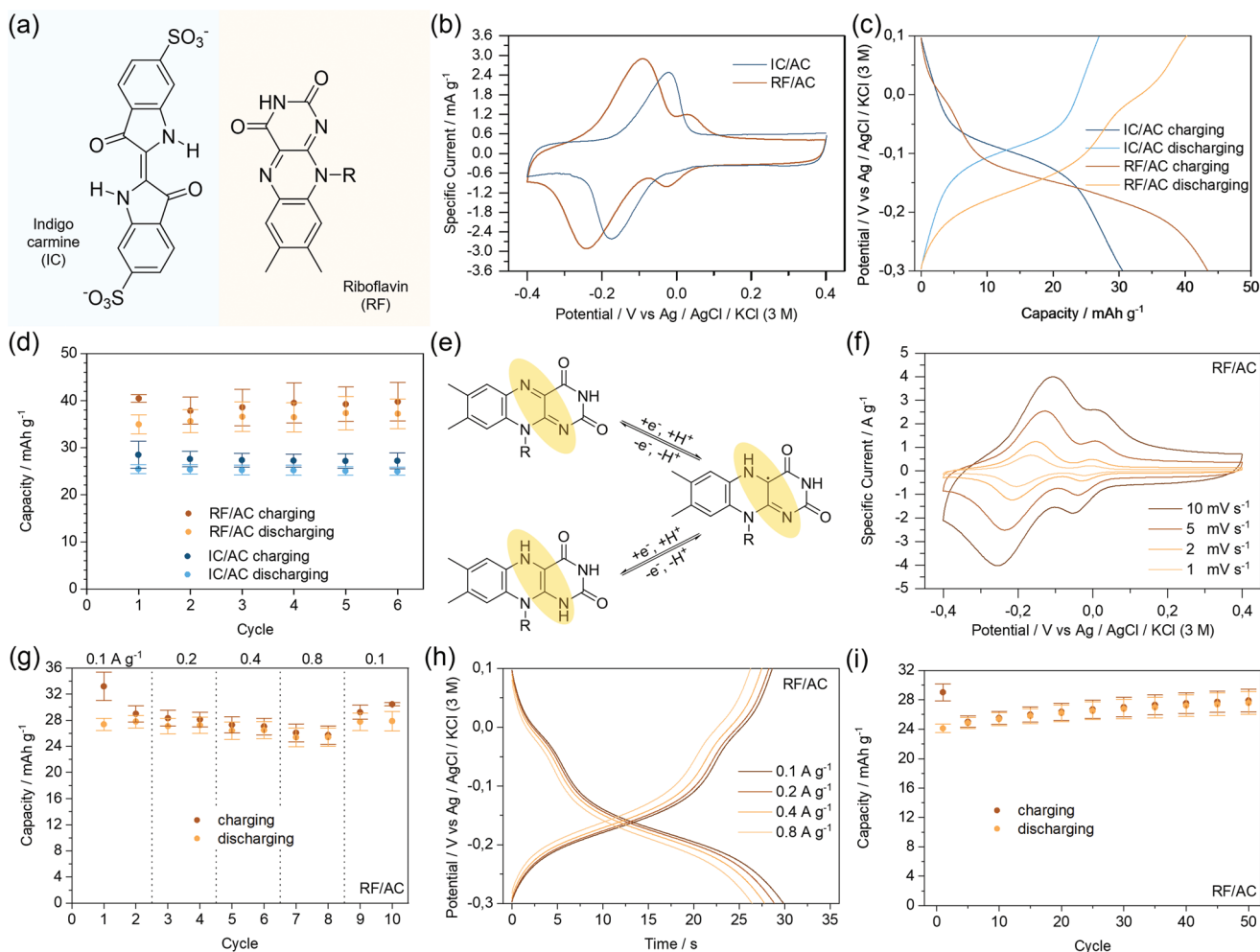


Figure 1. Tested anode materials. a) IC and RF, the food additives tested as potential anode materials. All the measurements were performed with the composites of small molecules, IC and RF mixed with AC. b) Cyclic voltammogram of IC/AC and RF/AC composites at 5 mV s^{-1} . c) Galvanostatic charging-discharging curve of IC/AC and RF/AC composites at 0.1 A g^{-1} . d) Galvanostatic charging-discharging capacities of IC/AC and RF/AC composites at 0.1 A g^{-1} . e) Proposed mechanism of RF redox reaction. (f) Cyclic voltammograms of RF/AC at different scan rates. g) Galvanostatic charging-discharging capacities of RF/AC composite at different charging rates. h) Corresponding galvanostatic charging-discharging curves. i) Capacities of RF/AC composite as determined by galvanostatic charging-discharging measurements at 0.8 A g^{-1} .

The electrolyte of choice in this work is a 1 M aqueous solution of sodium hydrogen sulfate (NaHSO_4 , E 514(ii)), since it is an edible salt with slight acidity, meaning that the protons, the cations with the highest mobility in water, are used to transport charge.

Cyclic voltammograms of IC/AC and RF/AC (Figure 1b) show the redox reactions occurring at around -0.1 V and (dominant) -0.15 V versus Ag/AgCl in KCl (3 M), in the following text shortened as versus Ag, respectively. The IC undergoes the one-step two-electron reduction process, as reported in literature,^[29] while RF undergoes the reduction in two steps. The galvanostatic charging-discharging curves (Figure 1c) confirm the observed trends, with the plateaus occurring at the aforementioned potentials. The charging-discharging capacities of IC/AC and RF/AC do not show significant degradation during 6 cycles (Figure 1d), with discharging capacities of ≈ 26 and 36 mAh g^{-1} for IC/AC and RF/AC, respectively. The higher discharge capacity of RF/AC and the lower potential of the dominant

peak/plateau made it the preferred choice for the anode. The cyclic voltammogram of AC is purely rectangular, and the galvanostatic charging-discharging curves are sloping lines with no plateau (Figure S4, Supporting Information). This indicates that the RF- and IC-based electrodes exhibit redox behavior that comes from small molecules, along with a small amount of capacitive behavior coming from the carbon. By considering the galvanostatic charging-discharging capacity of carbon to be 11 mAh g^{-1} , we estimated the RF/AC composite exhibits more than 90% of the RF theoretical capacity (details of the calculation can be found in Supporting Information – 5. Electrochemical measurements details).

The two-step redox reaction of RF is proposed in Figure 1e. Although the main cation in the electrolyte is a proton, RF does not undergo a one-step two-electron process, characteristic for dissolved RF. This behavior can be ascribed to immobilization of RF on the surface, as described in previous report.^[30] The cyclic voltammograms of RF/AC at lower scan rates (Figure 1f)

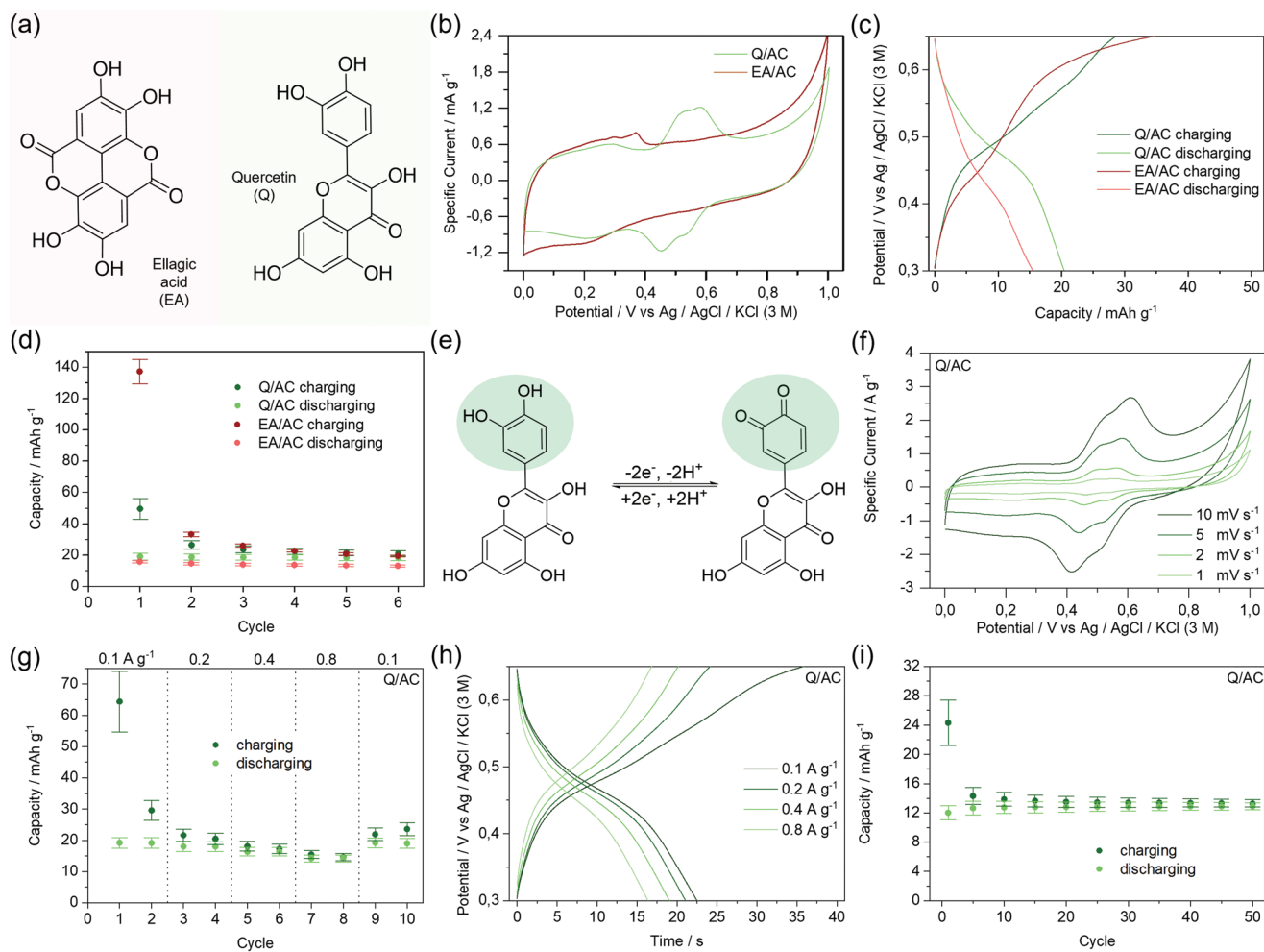


Figure 2. Tested cathode materials. a) EA and Q, the food ingredients tested as potential cathode materials. All the measurements were performed with the composites of small molecules, EA and Q mixed with AC. b) Cyclic voltammogram of EA/AC and Q/AC composites at 5 mV s^{-1} . c) Galvanostatic charging-discharging curve of EA/AC and Q/AC composites at 0.1 A g^{-1} . d) Galvanostatic charging-discharging capacities of EA/AC and Q/AC composites at 0.1 A g^{-1} . e) Proposed redox mechanism of Q. f) Cyclic voltammograms of Q/AC composite at different scan rates. g) Galvanostatic charging-discharging capacities of Q/AC composite at different charging rates. h) Corresponding galvanostatic charging-discharging curves. i) Capacities of Q/AC composite as determined by galvanostatic charging-discharging measurements at 0.8 A g^{-1} .

confirm the previous assumption of the two-step process. Intriguingly, the RF/AC shows excellent capacity retention with the increasing charging rate (Figure 1g,h), showing that fast charging of these materials is possible. Furthermore, RF/AC shows a slight increase in the capacity during 50 charging-discharging cycles at 0.8 A g^{-1} (Figure 1i), reaching $\approx 25 \text{ mAh g}^{-1}$. The effect is ascribed to the rearrangements in the material during charging-discharging, which causes better availability of the redox centers. The efficiency during these 50 cycles remains high, above 98% (Figure S5, Supporting Information).

EA and Q were the two food ingredients tested as cathode materials (Figure 2a). To our knowledge, neither of these materials were previously tested as active materials in batteries. However, the redox-active behavior of catecholic groups, which both compounds contain, in acidic electrolytes has been well described in the literature.^[32–35] Catecholic groups can be reversibly oxidized, forming *o*-quinones. As this reaction occurs at high potentials compared to other organic molecules, it

is suitable as a cathode reaction.^[36] While, to our knowledge, EA and Q do not take part in biological redox reactions, there are similar molecules that do. For example, the *p*-quinone and *p*-hydroquinone redox pair can be found in ubiquinones (coenzymes Q), which are common redox co-factors found in nature.^[37]

While Q/AC shows redox activity around 0.5 V versus Ag, in agreement with previous literature,^[38] no reversible redox activity of EA/AC can be observed (Figure 2b). During the first cycle of EA/AC, an irreversible oxidation peak can be observed (Figure S6, Supporting Information), indicating that it is redox-active, but irreversible. As EA has two catecholic centers, we postulate that the oxidized product loses aromaticity and, therefore, gets washed away as the π - π interactions with the activated carbon surface become weak.^[39] Galvanostatic charging-discharging cycles confirm this behavior, as the plateau around 0.5 V versus Ag is visible for Q/AC, while no plateau is observed for EA/AC (Figure 2c). The galvanostatic charging-discharging

measurements point to a much higher charging than discharging capacity during the first cycle not only for EA/AC but also for Q/AC (Figure 2d). Compared to the pure AC electrodes (Figure S7, Supporting Information), a pronounced set of peaks and plateaus around 0.5 V versus Ag region of galvanostatic charging-discharging curves. Furthermore, the first high charging capacity of Q/AC electrodes can be ascribed to the AC, as the same effect is visible during the first charging cycle of the pure AC (Figure S7c, Supporting Information). The Q/AC shows a discharge capacity of $\approx 18 \text{ mAh g}^{-1}$, while the AC shows $\approx 10 \text{ mAh g}^{-1}$. About 28% of the theoretical capacity of Q is used in the Q/AC composite (details of the calculation can be found in Supporting Information –5. Electrochemical measurements details). Q/AC was taken as the cathode material of choice for the edible battery.

Since, to our knowledge, the redox mechanism of Q has not been studied before, we propose a mechanism based on similar catechol-containing redox-active materials (Figure 2e).^[32,40,41] During oxidation, the catechol transforms into the *o*-quinone in a one-step two-electron process, while the opposite occurs during reduction. The cyclic voltammograms of the Q/AC composite at varying scan rates indicate a redox reaction occurring around 0.5 V versus Ag (Figure 2f). The galvanostatic charging-discharging measurements at different charging rates show a rather stable discharge capacity (Figure 2g). The capacity retention is high, dropping from around 19 mAh g^{-1} at 0.1 A g^{-1} to 14 mAh g^{-1} at 0.8 A g^{-1} . Charging-discharging curves confirm a redox reaction at $\approx 0.5 \text{ V}$ versus Ag (Figure 2h). The discharge capacity slightly rises during the first 50 cycles from ≈ 12 to 13 mAh g^{-1} at 0.8 A g^{-1} (Figure 2i), suggesting a similar rearrangement mechanism as that observed for RF/AC. After the first charging-discharging cycle, which involves an

initial oxidation and capacity loss as described previously, the efficiency quickly stabilizes above 95% (Figure S8, Supporting Information), indicating good cyclability of the material.

The final design of the edible battery included RF/AC and Q/AC composites as the anode and cathode, respectively. Full battery tests were performed by immersing the two electrodes in the electrolyte, a 1 M aqueous solution of NaHSO_4 , inside a plastic container.

The anode was loaded with 0.75 mg of RF/AC, while the cathode was loaded with 0.6 mg of Q/AC. The difference in anode and cathode loading was employed to balance the higher first charging capacity of Q/AC compared to RF/AC (Figure 1d and Figure 2d). The full battery was assembled in the discharged state. It is difficult to find a pair of edible molecules that can give energy spontaneously, without charging. Such two molecules would react thermodynamically in the nature, releasing the energy as heat. During charging, the Q underwent oxidation, while the RF was reduced (Figure 3a).

The cyclic voltammetry of the battery shows clear redox activity around 0.7 V versus RF (Figure 3b). Such results consist of the sum of the anode and cathode voltage obtained (-0.15 and 0.5 V versus Ag). Both anode and cathode showed good rate capability, reflected by the discharge capacity of the full battery dropping from 22 to just 18 mAh g^{-1} while the charging rate increased from 0.1 to 0.8 A g^{-1} (Figure 3c).

The corresponding charging-discharging curves indicate the charging plateau at $\approx 0.75 \text{ V}$ versus RF and the discharging plateau at $\approx 0.65 \text{ V}$ versus RF (Figure 3d). The overall curves show a significant contribution to the capacitive behavior from activated carbon, characterized by sloping potential. The sloping potential is particularly significant above 0.8 and under 0.6 V versus RF. Therefore, long-term measurements were only

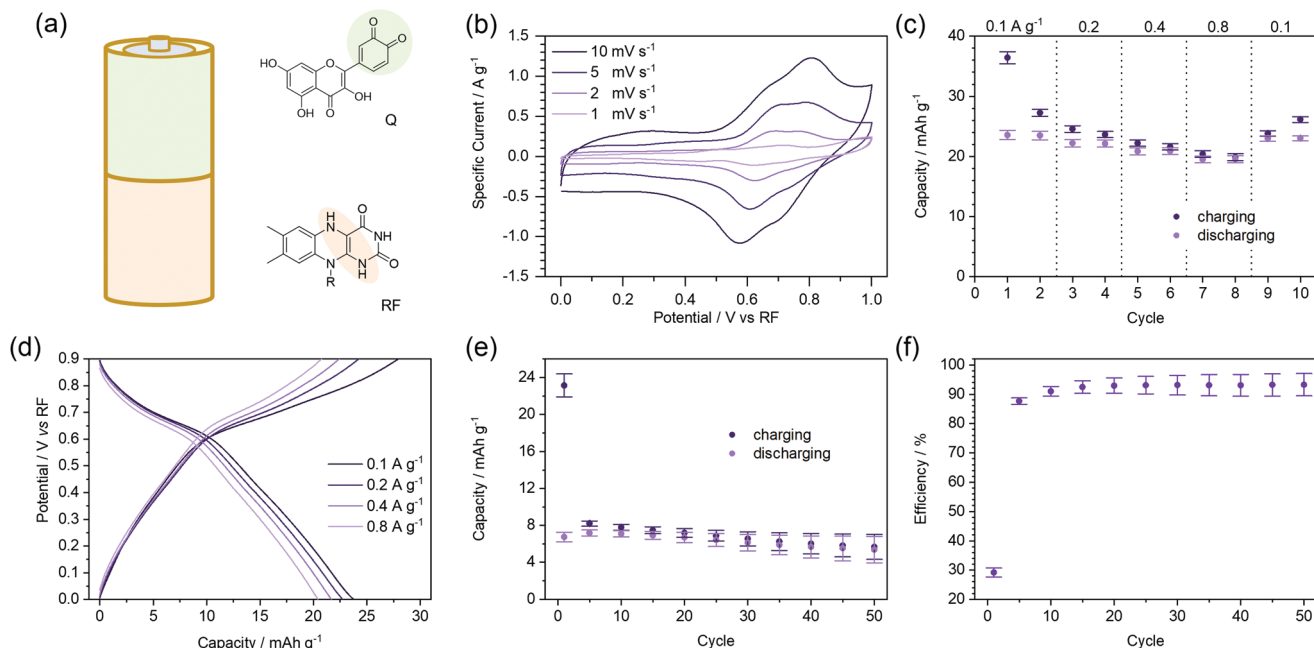


Figure 3. Full battery test with Q/AC composite as the cathode and RF/AC composite as the anode. a) Scheme of charged battery with oxidized Q and reduced RF. b) Cyclic voltammetry of the full battery at different scan rates. c) Galvanostatic charging-discharging capacities of the full battery at different charging rates. d) Corresponding galvanostatic charging-discharging curves. e) Galvanostatic charging-discharging capacities of the full battery at 0.4 A g^{-1} , charged to 0.8 V and then discharged to 0.6 V . f) Corresponding efficiencies.

performed by cycling the battery from 0.8 and down to 0.6 V (Figure 3e). This is a common practice in commercial batteries, such as those based on Li-ion technology, as the potential provided by the battery should be rather stable and discharging at too low of a potential or charging at too high of a potential can irreversibly damage the battery cell. While voltage between 0.6 and 0.8 V might seem low compared to commercial Li-ion battery, which usually have operating voltage above 3 V, such low voltages are appropriate to power edible devices. Ingestion of batteries (usually among children) is a well known problem which can cause serious tissue damage or even death, primarily as immersion in the body fluids produces a current flow, causing water electrolysis.^[42,43] Therefore, we find it advisable to keep the voltage of edible batteries well under 1.23 V, the minimum voltage needed for electrolysis of water.^[44]

During tests in which the battery was fully discharged to 0 V, the capacity in initial charging cycle was found to be 3 times higher than the discharge capacity of the subsequent cycle. In the subsequent cycles, the efficiency was rather high, 97% after 50 cycles (Figure 3f). While the discharge capacity rises within the first few cycles, up to 7.2 mAh g⁻¹ after 5 cycles, it drops to 5.4 mAh g⁻¹ after 50 cycles, likely due to the dissolution of the small molecules and the corresponding charged species.

So far, we have described the full battery realized using food supplement RF and Q as anode and cathode active materials, respectively. However, for an actual application of this technology, the design and implementation of a portable, potentially scalable, downsized, and robust device for an adequate amount of time is needed. In particular, all the components of a battery, including separator and packaging, have to be replaced with edible materials. To pursue this objective, the active material was deposited on gold-laminated ethyl cellulose, which served as current collector, just as in the case of the full battery (Figure 3). The loading amount was 1.5 mg for the RF/AC composite, and 1.2 mg for the Q/AC composite spread over 1 cm². Rather than submerging the electrodes in a plastic container filled with the electrolyte, the battery packaging was prepared from beeswax, while nori algae was used as the separator (Figure 4a; Figure S9, Supporting Information). The aqueous solution of NaHSO₄ electrolyte was not changed, but it was used in a significantly smaller amount (≈300 μL). Nori algae was soaked in the electrolyte and placed on the current collectors with pre-deposited small amount of electrolyte.

The cell was tested in galvanostatic charging-discharging at 240 μA by cycling between 0.6 and 0.8 V. The discharge capacity rises initially during the first 50 cycles from 6.3 to 7.0 μAh and afterward remains constant (Figure 4b). This can be ascribed to the wetting of the electrode, as the electrolyte reaches the greater surface area of the electrode. As previously observed, a plateau during discharge is visible at ≈0.65 V, and it takes ≈2 min to charge and discharge the cell (Figure 4c). The efficiency of the cell rises during cycling, reaching the value of 96.6% after 100 cycles (Figure S10a, Supporting Information). The same experiment was also performed at a lower current, 48 μA, resulting in a higher discharge capacity, ≈10 μAh (Figure 4d). A higher discharge capacity is expected as both cathode and anode showed significantly higher capacities at lower charging rates. The capacity decays from 10.1 to 9.1 μAh after 18 cycles. The profile of the charging-discharging curve is similar to the

one previously shown, with ≈13 min needed for the complete charging and ≈12 min for the full discharge (Figure 4e). The efficiency rises during cycling, reaching 86.9% after 18 cycles (Figure S10b, Supporting Information). The formed battery cell is fully edible as all the ingredients in the cell are significantly under the daily recommended limit (Figure 4f; Table S2, Supporting Information). Changes during cycling were investigated using electrochemical impedance spectroscopy (EIS). The Nyquist plot (Figure S11, Supporting Information) of the pristine electrodes shows two semicircles, indicating two interfaces in the battery. However, while the resistance of the first interface does not change during cycling, the resistance of the second interface increases. Nevertheless, the morphology of the electrodes does not get significantly changed upon cycling (Figure S12, Supporting Information). Therefore, we hypothesize that the second interface forms as the thin gold layer gets damaged, a process that could be significantly reduced by automated production of edible gold electrodes. Alternatively, it is possible that the second interface forms as a result of processes inside the electrode structure, not visible in SEM.

To prove that such an edible battery can power electronics, we connected two batteries in series to power an LED (HLMPK150 by Broadcom). Upon charging, the batteries provided the power needed to illuminate the LED (Figure 4g; Video S1, Supporting Information), proving that they are suitable as a power source.

The development of printable redox inks in the future would pave the way for improved designs of similar edible batteries, significantly enhancing the figure of merit of edible power sources.

3. Conclusion

In this work, we realized a fully edible rechargeable battery for the first time, which can be used to power edible electronics. Redox-active riboflavin and quercetin were first incorporated in composites with activated carbon to ensure free electrons flow from and to the redox centers. The composites were deposited on gold edible current collectors and bound with ethyl cellulose. The battery was closed with a nori algae separator soaked with 1 M aqueous solution of sodium hydrogen sulfate. The electrochemical performances of anode, cathode, and battery were studied in detail. The riboflavin anode composite showed clear redox activity with a discharge capacity up to 36 mAh g⁻¹, while the quercetin cathode composite reached 18 mAh g⁻¹. Riboflavin redox activity occurred 0.7 V lower than quercetin, and the full battery was assembled using these components as an anode and a cathode, respectively. The full battery demonstrated a discharging plateau at ≈0.65 V and capacity of up to 7.2 mAh g⁻¹. Lastly, a potentially scalable proof-of-principle edible battery has been realized by encapsulating the anode and cathode with edible beeswax. These proof-of-principle batteries showed pronounced redox behavior at 0.65 V, and capacity of up to 10 μAh, which can generate 48 μA for >12 min exploiting a cell with an active area of 1 cm². The bulky battery housing used in this proof-of-concept device is currently not suitable for real applications. Therefore, thinner and flexible edible housings are to be developed in the future, for example mimicking the pouch housing used in commercial batteries. Additionally, the flexibility of our edible battery

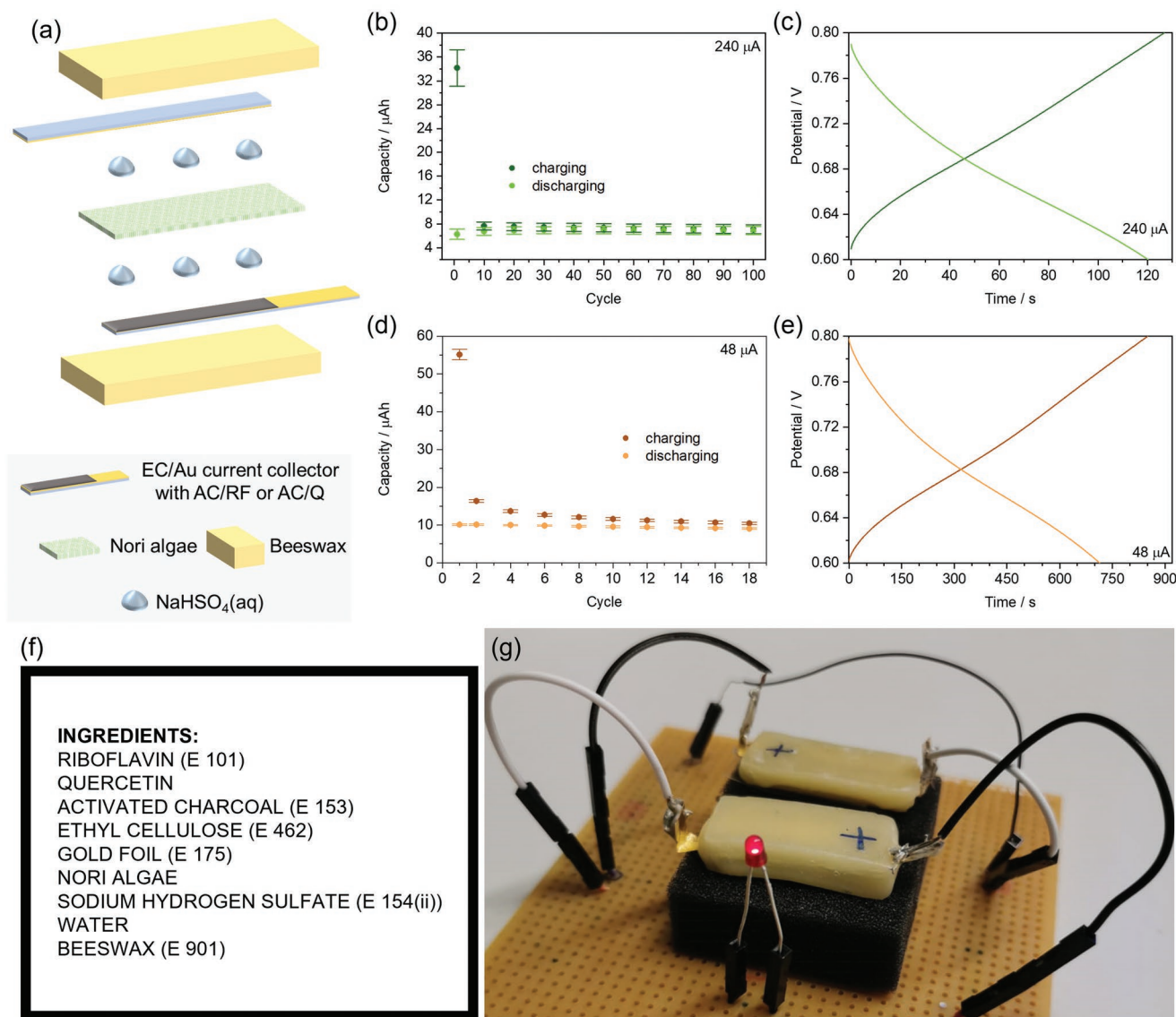


Figure 4. Fully edible battery cell. a) A fully edible battery was assembled using beeswax as packing, gold-laminated ethyl cellulose (EC/Au) as current collector, RF/AC or Q/AC composite as electrode material, the aqueous solution of NaHSO₄ as electrolyte, and nori algae as separator. b) Galvanostatic charging–discharging capacities for 100 cycles at a current of 240 μA. c) Corresponding charging–discharging curves. d) Galvanostatic charging–discharging capacities for 18 cycles at a current of 48 μA. e) Corresponding charging–discharging curves. f) List of ingredients found in a fully edible battery cell. g) An LED powered by two edible cells connected in series.

electrodes can be exploited to further reduce the battery volume for a given capacity, thus allowing to place the battery in a pill or other easily ingestible containers.

Furthermore, it was shown these batteries can power simple low-power off-the-shelf electronic components, such as a light-emitting diode. An easily implementable edible battery, such as the one demonstrated here, is poised to unlock a vast number of applications in healthcare, pharmacology, and food science, boosting the transition from ingestible to fully edible technologies and devices. However, in the short term it could also replace the toxic battery technologies currently used in ingestible electronic devices. The battery demonstrated a stable operating potential compared to the previously reported edible supercapacitors, a higher operating potential compared

to previously reported edible fuel cell, and it is a fully edible rechargeable device compared to the previous report of the edible battery electrode materials.

Supporting Information

Supporting Information is available from the Wiley Online Library or from the author.

Acknowledgements

The authors would like to thank Simone Lauciello for the help with energy dispersive X-Ray analysis and Nathan Pataki for copyediting the

manuscript. Furthermore, Nagaraj Patil, Rebeca Marcilla, and Mirko Prato are thanked for fruitful discussions. L.L., P.C., I.K.I., and M.C. acknowledge the support of the European Research Council (ERC) under the European Union Horizon 2020 research and innovation programme within the project “ELFO”, Grant Agreement No. 864299. V.G., V.F.A., and M.C. acknowledge the support from the European Union Horizon 2020 research and innovation programme within the FET project “ROBOFOOD”, Grant Agreement No. 964596. P.C. acknowledges funding from the Marie Skłodowska-Curie actions (project name: BioConTact, grant agreement No. 101022279) under the European Union Horizon 2020 research and innovation programme. This work also received support from the European Union Horizon 2020 research and innovation programme within the project “GREENELIT”, Grant Agreement No. 951747, and falls within the Sustainability Initiative of Istituto Italiano di Tecnologia.

Open access funding provided by Istituto Italiano di Tecnologia within the CRUI-CARE agreement.

Conflict of Interest

The authors declare no conflict of interest.

Data Availability Statement

The data that support the findings of this study are available from the corresponding author upon reasonable request.

Keywords

activated carbon, edible electronics, energy storage, green chemistry, green electronics, sustainability

Received: December 6, 2022

Revised: March 2, 2023

Published online:

- [1] E. M. Crimmins, *Gerontologist* **2015**, *55*, 901.
- [2] N. Zmora, J. Suez, E. Elinav, *Nat. Rev. Gastroenterol. Hepatol.* **2019**, *16*, 35.
- [3] L. A. Beardslee, G. E. Banis, S. Chu, S. Liu, A. A. Chapin, J. M. Stine, P. J. Pasricha, R. Ghodssi, *ACS Sens.* **2020**, *5*, 891.
- [4] A. S. Sharova, F. Melloni, G. Lanzani, C. J. Bettinger, M. Caironi, *Adv. Mater. Technol.* **2021**, *6*, 2000757.
- [5] M. Irimia-Vladu, E. D. Głowacki, G. Voss, S. Bauer, N. S. Sariciftci, *Mater. Today* **2012**, *15*, 340.
- [6] M. Irimia-Vladu, *Chem. Soc. Rev.* **2014**, *43*, 588.
- [7] P. Cataldi, L. Lamanna, C. Bertei, F. Arena, P. Rossi, M. Liu, F. Di Fonzo, D. G. Papageorgiou, A. Luzio, M. Caironi, *Adv. Funct. Mater.* **2022**, *32*, 2113417.
- [8] J. Kim, I. Jeerapan, B. Ciui, M. C. Hartel, A. Martin, J. Wang, *Adv. Healthcare Mater.* **2017**, *6*, 1700770.
- [9] W. Xu, H. Yang, W. Zeng, T. Houghton, X. Wang, R. Murthy, H. Kim, Y. Lin, M. Mignolet, H. Duan, H. Yu, M. Slepian, H. Jiang, *Adv. Mater. Technol.* **2017**, *2*, 1700181.
- [10] I. K. Ilic, L. Lamanna, D. Cortecchia, P. Cataldi, A. Luzio, M. Caironi, *ACS Sens.* **2022**, *7*, 2995.
- [11] L. Lamanna, P. Cataldi, M. Friuli, C. Demitri, M. Caironi, *Adv. Mater. Technol.* **2022**, *8*, 2200731.
- [12] M. Irimia-Vladu, P. A. Troshin, M. Reisinger, L. Shmygleva, Y. Kanbur, G. Schwabegger, M. Bodea, R. Schwödiauer, A. Mumyatov, J. W. Fergus, V. F. Razumov, H. Sitter, N. S. Sariciftci, S. Bauer, *Adv. Funct. Mater.* **2010**, *20*, 4069.
- [13] M. Irimia-Vladu, E. D. Głowacki, P. A. Troshin, G. Schwabegger, L. Leonat, D. K. Suzarova, O. Krystal, M. Ullah, Y. Kanbur, M. A. Bodea, V. F. Razumov, H. Sitter, S. Bauer, N. S. Sariciftci, *Adv. Mater.* **2012**, *24*, 375.
- [14] A. S. Sharova, M. Caironi, *Adv. Mater.* **2021**, *33*, 2103183.
- [15] X. Wang, W. Xu, P. Chatterjee, C. Lv, J. Popovich, Z. Song, L. Dai, M. Y. S. Kalani, S. E. Haydel, H. Jiang, *Adv. Mater. Technol.* **2016**, *1*, 1600059.
- [16] C. Gao, C. Bai, J. Gao, Y. Xiao, Y. Han, A. Shaista, Y. Zhao, L. Qu, *J. Mater. Chem. A* **2020**, *8*, 4055.
- [17] Y. J. Kim, S. E. Chun, J. Whitacre, C. J. Bettinger, *J. Mater. Chem. B* **2013**, *1*, 3781.
- [18] I. Jeerapan, B. Ciui, I. Martin, C. Cristea, R. Sandulescu, J. Wang, *J. Mater. Chem. B* **2018**, *6*, 3571.
- [19] M. Winter, B. Barnett, K. Xu, *Chem. Rev.* **2018**, *118*, 11433.
- [20] L. A. Sazanov, *Nat. Rev. Mol. Cell Biol.* **2015**, *16*, 375.
- [21] Y. J. Kim, W. Wu, S. E. Chun, J. F. Whitacre, C. J. Bettinger, *Proc. Natl. Acad. Sci. USA* **2013**, *110*, 20912.
- [22] E. Panel, A. Nda, *EFSA J* **2013**, *11*, 3419.
- [23] S. Opinion, *EFSA J* **2014**, *12*, 3808.
- [24] S. Opinion, *EFSA J* **2013**, *11*, 3449.
- [25] J. V. Formica, W. Regelson, *Food Chem. Toxicol.* **1995**, *33*, 1061.
- [26] J. M. Landete, *Food Res Int* **2011**, *44*, 1150.
- [27] H. K. Song, G. T. R. Palmore, *Adv. Mater.* **2006**, *18*, 1764.
- [28] M. Yao, K. Kuratani, T. Kojima, N. Takeichi, H. Senoh, T. Kiyobayashi, *Sci. Rep.* **2014**, *4*, 3650.
- [29] J. Carretero-González, E. Castillo-Martínez, M. Armand, *Energy Environ. Sci.* **2016**, *9*, 3521.
- [30] M. Lee, J. Hong, D. H. Seo, D. H. Nam, K. T. Nam, K. Kang, C. B. Park, *Angew. Chemie – Int. Ed.* **2013**, *52*, 8322.
- [31] A. Orita, M. G. Verde, M. Sakai, Y. S. Meng, *Nat. Commun.* **2016**, *7*, 13230.
- [32] G. Milczarek, O. Inganäs, *Science (80-)*. **2012**, *335*, 1468.
- [33] I. K. Ilic, M. Meurer, S. Chaleawler-Umporn, M. Antonietti, C. Liedel, *RSC Adv.* **2019**, *9*, 4591.
- [34] N. Patil, A. Mavrandonakis, C. Jérôme, C. Detrembleur, J. Palma, R. Marcilla, *ACS Appl. Energy Mater.* **2019**, *2*, 3035.
- [35] N. Patil, A. Mavrandonakis, C. Jérôme, C. Detrembleur, N. Casado, D. Mecerreyes, J. Palma, R. Marcilla, *J. Mater. Chem. A* **2021**, *9*, 505.
- [36] S. Muench, A. Wild, C. Friebe, B. Häupler, T. Janoschka, U. S. Schubert, *Chem. Rev.* **2016**, *116*, 9438.
- [37] D. B. Zorov, M. Juhaszova, S. J. Sollott, *Physiol. Rev.* **2014**, *94*, 909.
- [38] F. Villacañas, M. F. R. Pereira, J. J. M. Órfão, J. L. Figueiredo, *J. Colloid Interface Sci.* **2006**, *293*, 128.
- [39] A. M. O. Brett, M. E. Ghica, *Electroanalysis* **2003**, *15*, 1745.
- [40] F. N. Ajjan, M. J. Jafari, T. Rebiš, T. Ederth, O. Inganäs, *J. Mater. Chem. A* **2015**, *3*, 12927.
- [41] I. K. Ilic, M. Perovic, C. Liedel, *ChemSusChem* **2020**, *13*, 1856.
- [42] S. Chung, V. Forte, P. Campisi, *Clin Pediatr Emerg Med* **2010**, *11*, 225.
- [43] M. K. McConnell, *J Pediatr Nurs* **2013**, *28*, e42.
- [44] A. J. Shih, M. C. O. Monteiro, F. Dattila, D. Pavesi, M. Philips, A. H. M. da Silva, R. E. Vos, K. Ojha, S. Park, O. van der Heijden, G. Marcandalli, A. Goyal, M. Villalba, X. Chen, G. T. K. K. Gunasooriya, I. McCrum, R. Mom, N. López, M. T. M. Koper, *Nat. Rev. Methods Prim.* **2022**, *2*, 84.